

Synapse-specific regulation of AMPA receptor function by PSD-95

Jean-Claude Béïque, Da-Ting Lin, Myoung-Goo Kang, Hiro Aizawa, Kogo Takamiya, and Richard L. Huganir*

Department of Neuroscience, Johns Hopkins University School of Medicine and Howard Hughes Medical Institute, 725 North Wolfe Street, Baltimore, MD 21205

Contributed by Richard L. Huganir, October 2, 2006 (sent for review September 15, 2006)

PSD-95 is a major protein found in virtually all mature excitatory glutamatergic synapses in the brain. Here, we have addressed the role of PSD-95 in controlling glutamatergic synapse function by generating and characterizing a PSD-95 KO mouse. We found that the α -amino-3-hydroxy-5-methylisoxazole-4-propionic acid (AMPA) subtype of glutamate receptor (AMPA)-mediated synaptic transmission was reduced in these mice. Two-photon (2P) uncaging of MNI-glutamate onto individual spines suggested that the decrease in AMPAR function in the PSD-95 KO mouse stems from an increase in the proportion of "silent" synapses i.e., synapses containing *N*-methyl-D-aspartate (NMDA) receptors (NMDARs) but no AMPARs. Unexpectedly, the silent synapses in the KO mouse were located onto morphologically mature spines. We also observed that a significant population of synapses appeared unaffected by PSD-95 gene deletion, suggesting that the functional role of PSD-95 displays synapse-specificity. In addition, we report that the decay of NMDAR-mediated current was slower in KO mice: The contribution of NR2B subunit containing receptors to the NMDAR-mediated synaptic current was greater in KO mice. The greater occurrence of silent synapses might be related to the greater magnitude of potentiation after long-term potentiation induction observed in these mice. Together, these results suggest a synapse-specific role for PSD-95 in controlling synaptic function that is independent of spine morphology.

glutamate receptors | hippocampus | spines | synaptic transmission | two-photon uncaging

Glutamate, the major excitatory neurotransmitter in the brain, activates ionotropic glutamate receptors of the α -amino-3-hydroxy-5-methylisoxazole-4-propionic acid (AMPA), *N*-methyl-D-aspartate (NMDA), and kainate subtypes. There is considerable interest in elucidating the molecular mechanisms that controls synaptic targeting and trafficking of these receptors, in part because of their role in the induction and expression of various forms of synaptic plasticity (1). These receptors are imbedded in an electron-dense structure, the postsynaptic density (PSD), which is believed to contain key molecules involved in the regulation of glutamate receptor targeting and trafficking. PSD-95, a member of the membrane-associated guanylate kinase (MAGUK) superfamily of proteins, is a core component of the PSD and is thought to be important in the control of excitatory synapse function (2, 3). Because of its interaction with the cytoplasmic domains of NMDA receptor (NMDAR) subunits, it has long been suspected that PSD-95 might control the synaptic targeting of NMDARs (4, 5). However, more recent studies based on sustained or transient overexpression of PSD-95 in neurons have forced a reassessment of this view by suggesting that the primary role of PSD-95 is restricted to controlling AMPAR synaptic expression (6–10). Intriguingly, previous work on a PSD-95 KO mouse, reported no apparent changes in either AMPAR or NMDAR function (11). The interpretation of these data are, however, complicated by the fact that these PSD-95 KO mice still express, albeit at low levels, a functional truncated form of PSD-95 (7, 10).

Here, we have reexamined the role of PSD-95 in glutamatergic neurotransmission in the hippocampus by carrying out electrophysiological recordings in a mouse line carrying a complete *PSD-95* gene deletion. Our results outline a defect in AMPAR-mediated transmission in the hippocampus of the KO mice. This effect can fully be accounted for by the greater proportion of "silent" synapses found in KO mice as determined by two-photon (2P) uncaging of MNI-glutamate (MNI-GLU). Interestingly, the defect in AMPAR function induced by *PSD-95* gene deletion appeared to be restricted to only a subpopulation of synapses, thereby suggesting that PSD-95 displays synapse specificity in its actions. In addition, these silent synapses found in KO mice were observed on morphologically mature spines, suggesting that PSD-95 plays a distinct role in controlling glutamatergic synapse function and spine morphology.

Results

A previous study using gene targeting of the *PSD-95* gene resulted in the expression of a truncated form of PSD-95 that contained the N-terminal portion of PSD-95 including PDZ domains 1 and 2 (11). This truncated form has been shown to functionally mimic the effect of full length PSD-95 on AMPAR synaptic expression (7). To generate a complete KO and minimize the possibility of generating a functional *PSD-95* deletion, a targeting construct was designed to delete PDZ 1 and 2 and generate an out-of-frame *PSD-95* transcript (Fig. 5A, which is published as supporting information on the PNAS web site). By using this targeting construct, the *PSD-95* gene was disrupted by homologous recombination in embryonic stem cells. Proper targeting was confirmed by Southern blot analysis of genomic DNA using the probe depicted in Fig. 5B and by PCR analysis. Western blot analysis confirmed that PSD-95 protein was not expressed in *PSD-95*^{-/-} (KO) mice (Fig. 5C). Similar results were obtained with several PSD-95 antibodies (data not shown). No gross anatomical or obvious behavioral abnormalities were apparent in these mice.

The AMPAR to NMDAR Ratio of Excitatory Postsynaptic Currents Is Reduced in *PSD-95*^{-/-} Mice. To examine the effect of a complete PSD-95 KO on glutamatergic transmission, we first determined

Author contributions: J.-C.B. and D.-T.L. contributed equally to this work; J.-C.B., D.-T.L., K.T., and R.L.H. designed research; J.-C.B., D.-T.L., M.-G.K., and H.A. performed research; J.-C.B., D.-T.L., and K.T. contributed new reagents/analytic tools; J.-C.B., D.-T.L., and M.-G.K. analyzed data; and J.-C.B. and R.L.H. wrote the paper.

Conflict of interest statement: Under a licensing agreement between Upstate Group, Inc. and The Johns Hopkins University, R.L.H. is entitled to a share of royalties received by the University on sales of products described in this article. R.L.H. is a paid consultant to Upstate Group, Inc. The terms of this arrangement are being managed by The Johns Hopkins University in accordance with its conflict-of-interest policies.

Abbreviations: 2P, two-photon; AMPA, α -amino-3-hydroxy-5-methylisoxazole-4-propionic acid; AMPAR, AMPA receptor; DL-AP5, D(-)-2-amino-5-phosphonopivalic acid; EPSC, excitatory postsynaptic current; eEPSC, evoked EPSC; LTP, long-term potentiation; mEPSC, miniature EPSC; MNI-GLU, MNI-Glutamate, 4-methoxy-7-nitroindolyl-caged-glutamate; NMDA, *N*-methyl-D-aspartate; NMDAR, NMDA receptor; P(n), postnatal day (n); PSD, post synaptic density.

*To whom correspondence should be addressed. E-mail: rhuganir@jhmi.edu.

© 2006 by The National Academy of Sciences of the USA

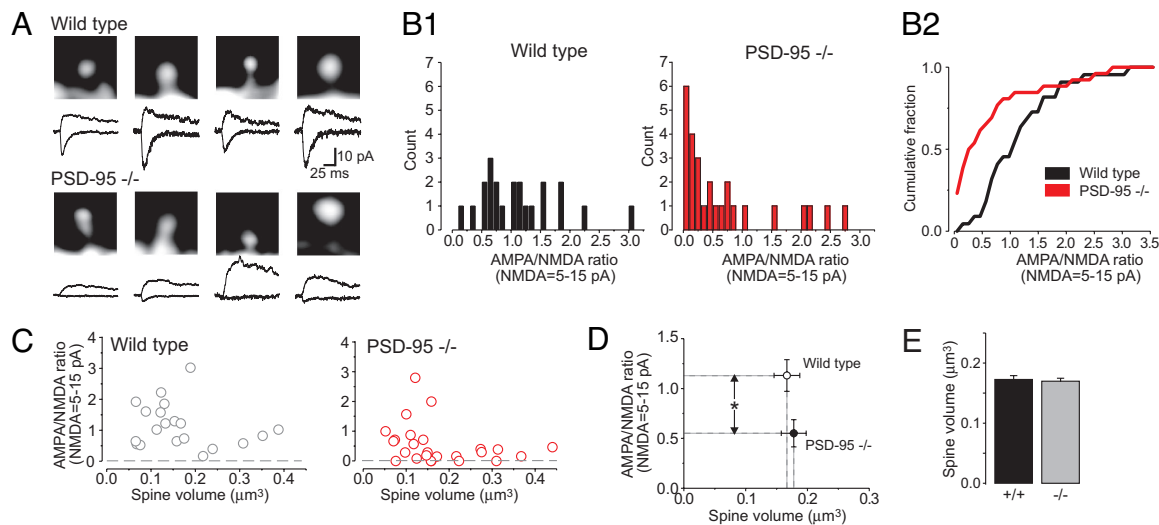


Fig. 3. Analysis of glutamatergic synapses by 2P uncaging of MNI-GLU and analysis of spine morphology in *PSD-95*^{-/-} mice. (A) Images of individual spines from WT and KO mice are shown with their respective 2P-EPSCs elicited at -70 and $+40$ mV. (B1) Distributions of 2P-AMPA/NMDA ratio onto individual spines are plotted for both WT and KO mice. (B2) Cumulative distribution plots of the ratios shown in B1. (C) The 2P-AMPA/NMDAR ratio obtained from uncaging onto individual spines is plotted against the volume of those spines. (D) The average AMPAR/NMDAR ratio (WT, 1.13 ± 0.14 , $n = 20$; KO, 0.63 ± 0.14 , $n = 26$; $P < 0.05$) obtained for individual spines by 2P-uncaging is plotted on the y axis against the average volume of the spines (WT, $0.16 \pm 0.02 \mu\text{m}^3$, $n = 20$; KO, $0.17 \pm 0.02 \mu\text{m}^3$, $n = 25$; $P = 0.7$) onto which the AMPAR/NMDAR were determined. (E) The volumes of spines were determined from a much broader population than in D; WT, $0.17 \pm 0.01 \mu\text{m}^3$, $n = 271$ spines, 7 cells, 4 mice; KO, $0.17 \pm 0.01 \mu\text{m}^3$, $n = 509$ spines, 12 neurons, 5 mice).

small, filopodia-like spines appeared to be largely devoid of AMPARs (Fig. 2F and ref. 18), although they expressed NMDAR-mediated dependent current (Fig. 2F). We thus hypothesized that the silent synapses observed in KO mice would predominantly be located on smaller, less developed, filopodia-like spines. To address this possibility, we plotted the AMPA/NMDA ratio obtained by 2P-uncaging for each spine against their respective volume (see *Supporting Methods*). In WT mice, we found that spine volume was not correlated with AMPA/NMDA ratios (Fig. 3C; $R^2 = 0.04$, $n = 20$). This lack of correlation was expected because these recordings were carried out in mice at an age (P13–P16) where AMPAR current was not correlated to spine volume (data not shown) and where silent synapses were not readily detected under our conditions (Fig. 3B). Interestingly, we also found that spine volume was not correlated with AMPA/NMDA ratio in the KO mice (Fig. 3C; $R^2 = 0.08$; $n = 25$). Closer examination revealed that the volume of spines that were found to be silent in KO mice spanned close to the entire range of spine volumes of the population. Thus, these results show that the silent synapses observed in KO mice are not restricted to smaller, less “developed” spines.

Although the results outlined above show that AMPA/NMDA ratios were not correlated to spine volume, it remains possible that there was a generalized reduction in spine volume in KO mice. For the spines from which we computed 2P-AMPA/NMDA ratios, we did not observe any significant difference in spine volume between WT and KO mice (Fig. 3C and D). To avoid a possible selection bias toward a morphologically homogenous population, we also determined spine volume from a much broader population of spines and also found that spine volumes were unchanged in KO mice (Fig. 3E). These results suggest that the general deficit in synaptic function observed after *PSD-95* gene deletion is not accompanied by any significant changes in the average spine volume. However, we observed a small but significant increase in spine length in the KO mice (see Fig. 9, which is published as supporting information on the PNAS web site).

Decay Kinetics of NMDAR-Mediated Synaptic Currents Are Slower in the *PSD-95*^{-/-} Mice. During the course of the experiments aimed at determining AMPA/NMDA ratio of eEPSCs at $+40$ mV (Fig.

1B and C), we noticed that the late portion of synaptic currents recorded at $+40$ mV (which predominantly reflects activation of NMDARs) tended to exhibit slower decay in the KO mice (time constants: WT, 78.2 ± 8.9 ms, $n = 17$; KO, 106.8 ± 7.1 ms, $n = 15$; $P < 0.05$; current decay fitted with a simple monoexponential). To address this issue more rigorously, we recorded isolated NMDAR-mediated synaptic currents (in 0.1 mM Mg^{2+} /10 mM glycine/10 μM NBQX; Fig. 4A). The isolated NMDAR synaptic currents in both WT and KO mice were best fitted by a double exponential decay (Fig. 10A, which is published as supporting information on the PNAS web site). As shown in Fig. 4B, the weighed time constant for NMDAR decay kinetics were significantly longer in KO compared with WT mice.

There are several mechanisms that could account for the longer NMDAR decay kinetics observed in KO mice. Studies in heterologous cells have shown that NMDA receptors containing NR2B subunits exhibit slower deactivation than those containing NR2A (19), raising the possibility that the longer decay kinetics observed in KO mice may reflect synaptic NMDAR of different subunit composition. The specific changes in decay kinetics of NMDAR-mediated currents (Fig. 10) are fully consistent with this idea (19). To further test this possibility, we determined the effects of the preferential NR2B-containing NMDAR antagonist ifenprodil on isolated NMDAR-mediated currents. We found that the inhibitory effect of ifenprodil ($3 \mu\text{M}$) on NMDAR-mediated currents was significantly greater in the KO mice, thereby suggesting that there is a greater contribution of NR2B subunit-containing NMDARs to the NMDAR-mediated synaptic current after *PSD-95* gene deletion (Fig. 4C).

Although our 2P-uncaging experiments were initially designed to determine AMPA/NMDA ratio at individual spines, we could get an estimate of NMDAR kinetics at single spines by fitting to a monoexponential decay of the NMDA portion of the 2P-EPSC at $+40$ mV. Consistent with our previous observations, we also found that the decay kinetics of 2P-NMDAR currents were significantly longer in the KO compared with WT mice (Fig. 4D and E).

There Was No Correlation Between NMDAR Kinetics and AMPAR Content at Individual Synapses. It has been well described that there is a gradual shift from mainly NR2B- to NR2A-containing

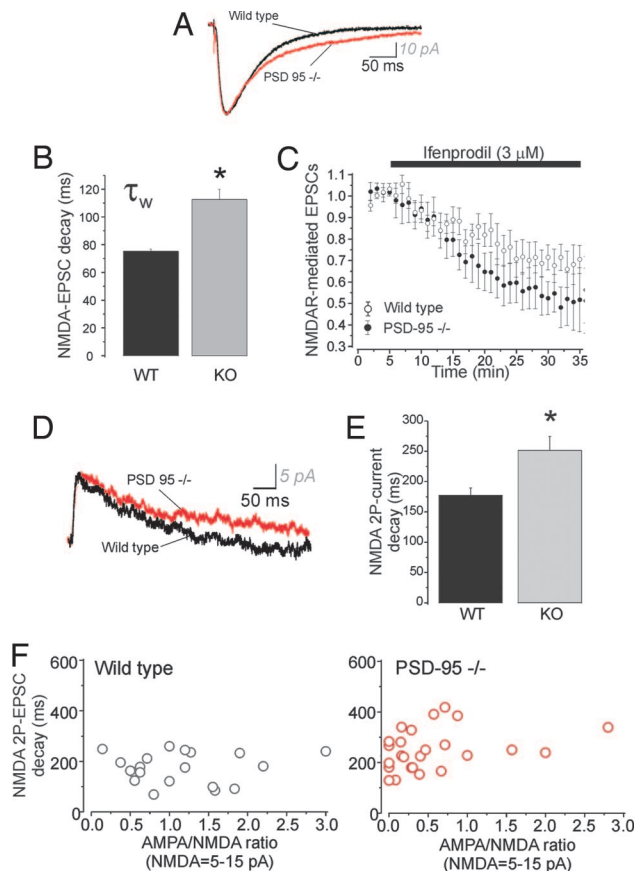


Fig. 4. Analysis of NMDAR function in *PSD-95*^{-/-} mice. (A) Current traces showing NMDAR-mediated synaptic currents recorded in 10 μ M glycine, 20 μ M NBQX, and 0.1 mM Mg^{2+} at -60 mV. (B) The decay kinetics of NMDAR-mediated synaptic currents were longer in KO mice (weighted time constants: WT, 75 ± 2 ms, $n = 8$; KO, 113 ± 7 ms, $n = 8$; $P < 0.01$). (C) The inhibition of NMDAR-mediated synaptic currents induced by ifenprodil (3 μ M) was larger in KO mice (WT, $n = 8$; KO, $n = 9$; $P < 0.05$, unpaired Student's *t* test tested between 30 and 35 min). Stimulation frequency was 0.06 Hz. (D) Current traces showing mixed AMPA and NMDA currents elicited by 2P-uncaging of MNI-GLU recorded in normal Ringer solution while holding the cell at $+40$ mV in WT and KO mice. (E) The decay kinetics of the NMDAR portion of the mixed 2P-current was approximated by fitting a single exponential decay and was longer in KO mice (WT, 173 ± 13 ms, $n = 20$; KO, 250 ± 16 ms; $n = 25$; $P < 0.01$). (F) The decay kinetics of the NMDAR portion of the current induced by 2P-uncaging of MNI-GLU (as determined in E) is plotted against the 2P-AMPA/NMDA ratio obtained from the same spines (elicited following the same procedure as in Fig. 3).

NMDARs during postnatal development (20, 21). In addition, the process of synaptic maturation is accompanied by the gradual incorporation of AMPARs into synapses (22). These studies raised the possibility that the incorporation of AMPARs in synapses would parallel the shift in NMDAR subunit composition from mainly NR2B-containing receptors toward NR2A-containing receptors and that these processes might be causally related. If this were the case, one would expect a tight correlation between the NR2 subunit composition of a given synapse and its AMPA receptor content. To address this issue, we plotted the AMPA/NMDA ratio of 2P-EPSCs against the decay kinetics of 2P-NMDAR-mediated responses at $+40$ mV for all spines analyzed (same as those in Fig. 3). Surprisingly, we found no correlation between AMPA/NMDAR ratio of 2P-EPSCs and 2P-NMDAR-mediated decay kinetics in both WT ($R^2 = 0.001$; $n = 20$) and in KO mice ($R^2 = 0.096$; $n = 26$). These results suggest that the level of AMPAR expression and the subunit

composition of NMDAR at individual synapses are not causally related. We also found no correlation between 2P-NMDAR-mediated decay kinetics and spine volume during this developmental period in both WT and KO mice (see Fig. 10B).

The Magnitude of Long-Term Potentiation (LTP) Is Greater in *PSD-95*^{-/-} Mice. To examine the functional consequences of the complete *PSD-95* KO on synaptic plasticity, we examined LTP in the CA1 region of the hippocampus using field potential recordings in the stratum radiatum. The magnitude of LTP, induced by delivering a θ burst-like protocol, was much greater in KO mice than in WT littermates (field EPSP slope, compared with baseline, at 30–40 min after LTP induction: WT, $182 \pm 13\%$; KO, $331 \pm 41\%$; Fig. 11, which is published as supporting information on the PNAS web site). This finding is similar to that reported for mice expressing the truncated form of *PSD-95* (11).

Discussion

PSD-95 and other members of the MAGUK superfamily of proteins are thought to be critical for the proper formation and maintenance of excitatory synapses. Using a combination of gene targeting, electrophysiological, and imaging approaches, we report that AMPAR function was impaired in *PSD-95* KO mice. Specifically, this reduction was caused by a greater proportion of synapses that lack functional AMPARs (i.e., silent synapses) rather than by a general decrease of functional AMPAR across all synapses. This finding suggests a synapse selectivity for *PSD-95*'s action. Our results further showed that silent synapses were found on morphologically mature spines in the KO mice. These results thus outline a distinct role of *PSD-95* in controlling glutamatergic synapse function independent of spine morphology. Moreover, in confirmation of a previous report, we find that disruption of the *PSD-95* gene results in a greater magnitude of LTP.

Complete genetic deletion of *PSD-95* leads, by approximately the 2nd week of life, to a reduction in the synaptic expression of AMPARs, but not NMDARs, as was apparent mainly from the observation that the reduction in the frequency of AMPAR-mediated mEPSCs in KO mice could quantitatively account for the reduction in AMPA/NMDA ratio. This finding obtained by using a loss-of-function strategy is conceptually consistent with studies showing that overexpression of *PSD-95* increases AMPAR function (6, 7, 9, 10). Interestingly, our 2P-uncaging experiments directly demonstrated a greater proportion of synapses that expressed NMDARs, and not AMPARs in the KO mice. These synapses are referred to as silent because NMDARs are nonfunctional at rest. The greater proportion of silent synapses in KO mice bears important consequences for synaptic plasticity because it is believed that silent synapses represent the preferential site of AMPAR insertion during LTP (23) (but see refs. 24 and 25). It is thus conceivable that the enhanced magnitude of LTP we observed in KO mice directly stems from the greater proportion of silent synapses. The corollary implication of these findings is that, whereas *PSD-95* appears to be a key molecule in controlling synaptic AMPARs expression, it does not appear to play an important role in the actual recruitment process of AMPARs to synapses during LTP.

In principle, the reduction in synaptic AMPAR function in KO mice could be caused by a decrease in synaptic expression of AMPARs across all synapses. Our results, however, support an alternate scenario whereby the deficit in synaptic AMPAR expression appears to be restricted to only a subset of synapses. Two independent sets of experiments lead to this interpretation. First, the amplitude of mEPSCs was unaltered by *PSD-95* gene deletion (there were simply fewer events). Second, the distribution of AMPA/NMDA ratios obtained from 2P-uncaging onto individual spines revealed that a subset of spines in KO mice displayed equally high ratios to those obtained from spines in WT mice. Together, these results suggest that a population of synapses have matured (at

least with respect to synaptic AMPAR insertion) normally in the absence of PSD-95. These results therefore suggest an intriguing selectivity in the actions of PSD-95 toward a specific population of synapses. Whether this apparent specificity reflects a function inherent to PSD-95 or rather a compensatory mechanism after PSD-95 genetic deletion is unclear. Other members of the MAGUK superfamily of proteins might be compensating for the lack of PSD-95 in a subset of synapses.

The decay kinetics of NMDAR currents were slower in KO mice. This effect can be accounted for, at least in part, by a greater synaptic expression of NR2B-containing NMDAR. In particular, our results suggest that the normal, developmentally regulated, switch of primarily NR2B- to NR2A-containing synaptic NMDAR is hindered in KO mice. Interestingly, the subunit composition of NMDARs has been suggested to decisively impact the polarity of synaptic plasticity, although contradictory findings are found in the literature (26–30). Because LTP is greater, and NMDARs containing the NR2B subunit appear to dominate in the KO mice, our results are broadly consistent with the idea that NR2B-containing NMDARs preferentially trigger LTP (27). However, we did not find any evidence that the silent synapses found in KO mice were enriched in NR2B-containing NMDARs. Because LTP is believed to be preferentially induced on silent synapses (15, 16, 23), these findings do not support the idea that NR2B-containing NMDARs preferentially link to the induction of LTP in KO mice. However, it is possible that spines with higher NR2B-containing NMDAR in KO mice are the ones that are more amenable to LTP regardless of their initial AMPAR content (i.e., regardless of whether they are silent or not) in KO mice. Our difficulty in inducing reliable LTP by 2P-uncaging unfortunately precluded us from directly testing these possibilities at this point.

Because thin, filopodia-like spines express less AMPARs on their surface than larger, more mature dendritic spines (18), we had initially hypothesized that the silent synapses observed in KO mice would preferentially be located on smaller spines. However, combined 2P-uncaging and spine morphological analysis revealed not only that spine volume were unchanged in KO mice but also that the silent synapses encountered in these mice were distributed on spines independently of their volume. These data thus suggest that synapse functional maturation and spine morphological development can be dissociated.

The number of AMPARs expressed at synaptic sites is believed to be governed by both activity-dependent (mainly NMDAR-dependent) and activity-independent processes (22, 26, 31, 32). Although results from this and other studies (6, 8–10) converge in showing that synaptic AMPARs are controlled by PSD-95, the molecular details of this effect are still unclear. First, the enhancement of AMPAR function by transient overexpression of PSD-95

does not require synaptic activity (10), thereby suggesting that this role of PSD-95 does not merely result from a general facilitatory action on NMDAR-dependent signaling. The observation that LTP was not abolished (it was actually enhanced) in KO mice supports this view while also arguing against a direct role of PSD-95 in the recruitment process of AMPAR to synapses during NMDAR-dependent LTP. Yet, it was also found that the transient overexpression of PSD-95 mimicked and occluded LTP (6, 10), thereby suggesting that LTP and PSD-95 control synaptic AMPAR by common mechanisms. Thus, it appears that PSD-95 is sufficient, although clearly not necessary, to enhance AMPAR number at synapses. The data presented here demonstrate that PSD-95 plays a critical role in controlling AMPAR expression at a subset of synapses. It is difficult to infer from our data whether the lack of AMPAR at these synapses reflects a synaptic insertion deficit or rather a synaptic stabilization deficit. Because the actual process of insertion of AMPARs after an LTP protocol is not compromised in KO mice, it is possible that PSD-95 mainly plays a role in maintaining the stability of synaptic AMPARs.

Methods

Generation of PSD-95-Deficient Mouse. PSD-95 gene deletion was obtained by standard homologous recombination technique. For more details, see *Supporting Methods*.

Electrophysiology. Whole-cell recordings or field recordings were obtained in the CA1 region of rat or mice hippocampus (P7–P25). For more details, see *Supporting Methods*.

2P Uncaging and Imaging. Whole-cell recordings of CA1 pyramidal neurons were obtained by following standard procedures, except that intracellular solution was supplemented with 40 μ M Alexa Fluor 594 to outline neuronal morphology. Slices were bathed in normal Ringer's solution supplemented with MINI-GLU. A section of a neuron was imaged, and the tip of a spine was illuminated (0.8 msec) with a laser tuned at 720 nm while monitoring the electrophysiological responses. For more details, see *Supporting Methods*.

We thank Elise Shumsky and Dr. Zbigniew Iwinski (Carl Zeiss Micro-Imaging group) for their continuous technical assistance, Dr. Haruo Kasai (University of Tokyo, Tokyo, Japan) for helpful discussion on spine volume calculation, Jason Tien for invaluable expertise in developing the spine volume calculation algorithm, Dr. Gareth Thomas for critical reading of the manuscript, and Dr. James Trimmer (University of California, Davis, CA) for providing a series of anti-PSD-95 polyclonal antibodies. This work was supported by the Howard Hughes Medical Institutes (R.L.H.), by grants from the National Institutes of Health (to R.L.H.), the National Alliance for Research on Schizophrenia and Depression (to J.-C.B.), and the Mental Illness Research Association (to J.-C.B.).

- Malenka RC, Nicoll RA (1999) *Science* 285:1870–1874.
- Kornau HC, Schenker LT, Kennedy MB, Seeburg PH (1995) *Science* 269:1737–1740.
- Hunt CA, Schenker LJ, Kennedy MB (1996) *J Neurosci* 16:1380–1388.
- Sheng M, Wyssynski M (1997) *BioEssays* 19:847–853.
- Kennedy MB (1997) *Trends Neurosci* 20:264–268.
- Stein V, House DR, Brecht DS, Nicoll RA (2003) *J Neurosci* 23:5503–5506.
- Schnell E, Sizemore M, Karimzadegan S, Chen L, Brecht DS, Nicoll RA (2002) *Proc Natl Acad Sci USA* 99:13902–13907.
- El-Husseini AE, Schnell E, Chetkovich DM, Nicoll RA, Brecht DS (2000) *Science* 290:1364–1368.
- Beique JC, Andrade R (2003) *J Physiol* 546:859–867.
- Ehrlich I, Malinow R (2004) *J Neurosci* 24:916–927.
- Migaud M, Charlesworth P, Dempster M, Webster LC, Watabe AM, Makhinson M, He Y, Ramsay MF, Morris RG, Morrison JH, et al. (1998) *Nature* 396:433–439.
- Hsia AY, Malenka RC, Nicoll RA (1998) *J Neurophysiol* 79:2013–2024.
- Ungless MA, Whistler JL, Malenka RC, Bonci A (2001) *Nature* 411:583–587.
- Sans N, Petralia RS, Wang YX, Blahos J, II, Hell JW, Wenthold RJ (2000) *J Neurosci* 20:1260–1271.
- Liao D, Hessler NA, Malinow R (1995) *Nature* 375:400–404.
- Isaac JT, Nicoll RA, Malenka RC (1995) *Neuron* 15:427–434.
- Raastad M, Storm JF, Andersen P (1992) *Eur J Neurosci* 4:113–117.
- Matsuzaki M, Ellis-Davies GC, Nemoto T, Miyashita Y, Iino M, Kasai H (2001) *Nat Neurosci* 4:1086–1092.
- Vicini S, Wang JF, Li JH, Zhu WJ, Wang YH, Luo JH, Wolfe BB, Grayson DR (1998) *J Neurophysiol* 79:555–566.
- Flint AC, Maisch US, Weishaupt JH, Kriegstein AR, Monyer H (1997) *J Neurosci* 17:2469–2476.
- Williams K, Russell SL, Shen YM, Molinoff PB (1993) *Neuron* 10:267–278.
- Zhu JJ, Malinow R (2002) *Nat Neurosci* 5:513–514.
- Matsuzaki M, Honkura N, Ellis-Davies GC, Kasai H (2004) *Nature* 429:761–766.
- Kopec CD, Li B, Wei W, Boehm J, Malinow R (2006) *J Neurosci* 26:2000–2009.
- Bagal AA, Kao JP, Tang CM, Thompson SM (2005) *Proc Natl Acad Sci USA* 102:14434–14439.
- Barria A, Malinow R (2005) *Neuron* 48:289–301.
- Liu L, Wong TP, Pozza MF, Lingenhoechl K, Wang Y, Sheng M, Auberson YP, Wang YT (2004) *Science* 304:1021–1024.
- Massey PV, Johnson BE, Moulton PR, Auberson YP, Brown MW, Molnar E, Collingridge GL, Bashir ZI (2004) *J Neurosci* 24:7821–7828.
- Weitlauf C, Honse Y, Auberson YP, Mishina M, Lovinger DM, Winder DG (2005) *J Neurosci* 25:8386–8390.
- Berberich S, Punnakkal P, Jensen V, Pawlak V, Seeburg PH, Hvalby O, Kohr G (2005) *J Neurosci* 25:6907–6910.
- Turrigiano GG, Nelson SB (2004) *Nat Rev Neurosci* 5:97–107.
- Luthi A, Schwyzler L, Mateos JM, Gahwiler BH, McKinney RA (2001) *Nat Neurosci* 4:1102–1107.